Investigation on an all-optical intensity modulator based on an optical microfiber coupler

Yang Yu (于 洋)[1,2], Qiang Bian (卞 强)[1], Nan Zhang (张 楠)[3], Yang Lu (路 阳)[1], Xueliang Zhang (张学亮)[1,*], and Junbo Yang (杨俊波)[2]

[1]*College of Meteorology and Oceanology, National University of Defense Technology, Changsha 410073, China*
[2]*College of Liberal Arts and Sciences, National University of Defense Technology, Changsha 410073, China*
[3]*The Medical Engineering & Maintenance Center, Chinese PLA General Hospital, Beijing 100853, China*
*Corresponding author: xueliang.john@hotmail.com

An all-optical intensity modulator based on an optical microfiber coupler (OMC) is presented. The modulator works at 1550 nm wavelength and is modulated directly by heating the coupling region with 980 nm pump light injected through the coupling port of the OMC. The OMC is controlled to have at least a 30 mm long coupling region with diameter smaller than 8 μm, and the uniform waist region diameter is about 3 μm. This is helpful to ensure the optical modulation function based on the light induced thermal effect in the coupling region, while pump light is injected. The modulation response is measured to show good linearity when the 980 nm pump light has a lower intensity (with power below 2.5 mW), which proves that the OMC acts as an all-optical modulator. The bandwidth of the modulator can be at 0.2–50 kHz with the average power of the intensity-modulated pump light about 2 mW, which can be further improved by optimizing the design of the coupler. The demonstrated modulator may have potential value for the application in an all-optical integration system.

OCIS codes: 230.4000, 060.2370.
doi: 10.3788/COL201816.040605.

Optical modulators are one of the important components in optical systems, which are generally based on electro-optic effects, thermo-optic effects, nonlinear effects, and elastic-optic effects[1,2]. To meet the requirements of high-speed all-optical integrated systems, special waveguide structures should be designed to enhance the optical confinement and the interaction between light and waveguide materials[3–8]. For silicon optical waveguides, its manufacture conditions are very strict. Compared with silicon optical waveguides, optical microfibers (OMs) have a number of outstanding optical and mechanical properties, including low loss, strong confinement, etc[9–13]. Especially, OMs also provide a new way for the development of novel optical modulators[14–18]. For example, by using the large evanescent field of OM, the all-optical fiber modulator based on a stereo graphene-microfiber structure (GMF) was demonstrated (by combining OM and graphene together to be GMF)[14–17]. By using the large surface area to volume ratio and strong optical confinement of OM, an all-optical phase modulator based on the thermo-optic effect has been fabricated[18]. However, there remains a challenge to use a single-port microfiber in optical interconnections, of which the solution comes from the OM couplers (OMCs). For an OMC, the coupled region could be controlled from several to several tens of millimeters in length and sub-wavelength scale in diameter[19]. The research results show that the parameters of the OMC's coupled region are very sensitive to temperature and the refractive index, which has been used for sensing[20–23]. Therefore, if the light induced thermal effect in the OMC changes the refractive index and waveguide structure

of the coupled region, the output characteristics of the OMC will be changed. Here, we present an all-optical intensity modulator based an OMCs. We have demonstrated that, when an intensity-modulated 980 nm light is injected into the coupling region, the transmitted 1550 nm light is modulated due to the light induced thermal effect.

The OMC is fabricated with two twisted conventional fibers in the drawing system based on the improved flame-brushing method, according to the fabrication techniques of conventional fiber couplers and OMs[19]. The diameter of the OMC in the coupling region is controlled to be at about the micrometer level. In order to control the coupler parameters, an online transmitted light power monitoring system is set up. OMCs with different structures and transmission characteristics can be tapered by precise control of parameters, such as heating zone length, heating temperature, tapered velocity, cone angle, etc[24]. Figure 1 shows the schematic of the composite OMC, which contains two taper regions and a uniform waist region.

It has been studied that the doped optical fiber has a weak optical modulation ability due to the limited optical field area in the fiber (usually an 8–10 μm diameter in the core of a conventional single-mode fiber) and large thermal conduction volume (usually 125 μm diameter for a conventional single-mode fiber)[2]. An OM has a smaller diameter than a conventional doped fiber, and the optical field could be confined in the sub-wavelength scale, so it is helpful to improve the modulation efficiency[18]. If the OMC has a smaller diameter as an OM at the coupling region, the light induced thermal effect will be enhanced. The operation light transmission in the OMC will be
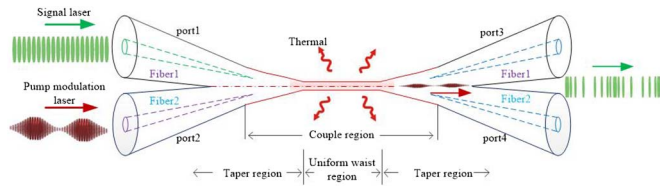
Fig. 1. Schematic illustration of the composite OMC and the all-optical modulation theory of the OMC.

modulated by the intensity modulation pump light heating the coupling region, and the all-optical modulation theory schematic illustration of the OMC is shown in Fig. 1.

In order to meet the optical modulation requirements, the OMC should have the coupling capability and maximally enhance the interaction between light and waveguide materials, as the coupling region of the OMC could be regarded as two OMs, which had been tightly adjacent. The study on all-optical phase modulators shows that the modulation efficiency is proportional to fiber length, and it is inverse to the fiber diameter in a certain range[2,18]. For the choice of the diameter of the modulated OM, the effective interaction area between light and fiber should be considered. For a SiO_2 OM, in order to confine 90% light energy inside the fiber, the diameter of the OM should be about 0.9 μm for a wavelength of 980 nm and about 1.4 μm for a wavelength of 1550 nm[25]. Such diameters could be considered as the optimal values at which the interactions between light and waveguide materials are the strongest. Taking into consideration the factors, such as manufacture techniques, transmission losses, and modulation stability, we have chosen the designed waist region diameter of the OM to be about 2 μm in the drawing system.

We have fabricated an OMC with the properties described above. A laser diode at 1550 nm wavelength is used as the light source of the OMC. The throughput port (Port3) and the coupling port (Port4) are monitored by two photodectors (OE-200). During the drawing process of the OMC, the output of Port3 is shown in Fig. 2(a). The x axis is the elongation length of the OMC. It can be noticed that when the elongation length is about 20 mm, the coupling effect begins to appear. With the
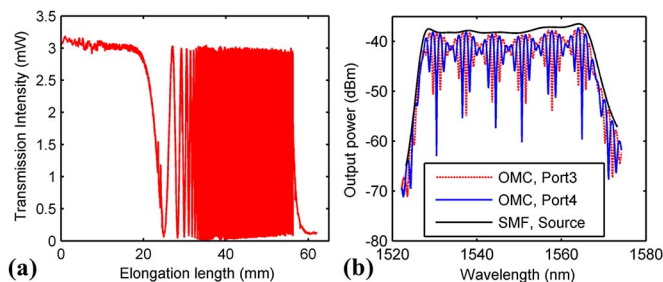

Fig. 2. (a) Transmission intensity of the microfiber coupler Port3 during the fabrication process. (b) Input and output optical spectra of the OMC.

elongation length increasing, the coupling efficiency is interchanging. When the designed OM diameter reached about 2 μm (corresponding to the 4 μm waist diameter of the coupling region of the OMC), which is given by the drawing system, we stopped the drawing process. The OMC has a coupling ratio of about 90%, and the transmission loss is less than 0.2 dB. The transmission loss includes absorption, scattering, etc[26]. A portion of the absorbed light will transform into heat, which is used for the modulation of the OMC properties.

Figure 2(b) shows the measured spectral characteristics of the OMC sample at output Port3 and Port4 by an optical spectrum analyzer with a spectral resolution of 0.01 nm. The coupled output is selective to wavelength, while the waist parameters are sensitive to external environmental parameters, such as refraction, temperature, and vibration, and could be used as sensors[20–23]. Figure 3 is the photograph of the OMC sample under an optical microscope. Due to the melting effect of the waist in the tapered process, the diameter of the uniform waist is about 3 μm.

According to the coupling theory, the light power of the two output ports can be expressed as[20–23]

$$P_3 l \; P_0 \cos^2 \left[\int_0^l Cz\mathrm{d}z \right], \tag{1}$$

$$P_4 l \; P_0 \sin^2 \left[\int_0^l Cz\mathrm{d}z \right], \tag{2}$$

where P_0 is incident operation light power, l is the length of the coupling region, and Cz is the coupling coefficient at location z. In order to enhance the influence of thermo-optic effect on the OMC coupled region, the OMC is required to have a tapered transition region and a uniform waist with a longer length and diameter below 8 μm. So, we set the uniform waist length as 10 mm and optimize the tapered angle parameters to ensure the total length of the transition region and uniform waist with the diameter below 8 μm to exceed 30 mm. In the other part of the tapered transition region in the OMC with a diameter larger than 8 μm, the transmission fundamental mode diameter is larger than in conventional fibers[25]. Consequently, the interaction between light and waveguide materials is weaker than in a conventional fiber, and the thermo-optic effect in this region could be ignored.

When the injected modulated pump light is injected with lower power, and the pump light can be expressed as $I_p \sin 2\pi f t$, the AC part of the output of the OMC can be expressed as[27]

Fig. 3. Image of the OMC in an optical microscope.

$$\Delta P_3 \quad -P_0 M L \frac{\eta \gamma \alpha I_p}{C \rho \pi r^2} \ \sin \pi f t, \tag{3}$$

$$\Delta P_4 \quad P_0 M L \frac{\eta \gamma \alpha I_p}{C \rho \pi r^2} \ \sin \pi f t, \tag{4}$$

where M is the coupling coefficient change rate caused by Δn, Δn is the change of the cladding refractive index by thermo-optic effect, L is the length of the OMC's uniform waist region, α is the loss coefficient of the OMC's uniform waist region, η is the fraction of the absorbed pump power that is turned into heat, and γ is thermo-optical coefficient. f is the refractive index modulation frequency (the pump light modulation frequency), r is the radius of the OMC's coupling fibers, and ρ and C are the density and specific heat of the OMC waveguide material (silica fiber). It can be seen that the modulation efficiency is in proportion to the length and the loss coefficient of the OMC's uniform waist region, and it is inversely proportional to the radius of the OMC couple fibers. At the same time, previous research results have shown that the modulation efficiency is inverse to the modulation frequency[18].

We set up an all-optical intensity modulation system to measure responses of OMC modulators driven by the intensity-modulated 980 nm light. An optical fiber generally shows absorption at a wide spectral range from ultraviolet to infrared wavelengths. The proposed modulation method exploits the light induced thermal effect and can be realized using light sources at other wavelengths as pump light. We used a light source at 980 nm just because it is widely used and easily available in labs.

The experimental configuration is illustrated in Fig. 4. The probe light is a 1550 nm semiconductor laser source (RIO, line width 2 kHz). It was injected into the OMC through an optical isolator. The 1550 nm output light of the OMC (Port3) was connected to a detector (New Focus, Model 1623) through a 980/1550 nm wavelength division multiplexer (WDM). The 980 nm pump laser was injected into the OMC through the coupling port (Port4). The WDM was also used to isolate the possibly coupled 980 nm light. The 980 nm pump laser was driven by a laser diode controller (ILX Light Wave LDC-37488B), which can modulate the output light by connecting a signal generator. Port2 of the OMC is inserted in a matching fluid through the fiber connector (FC) for
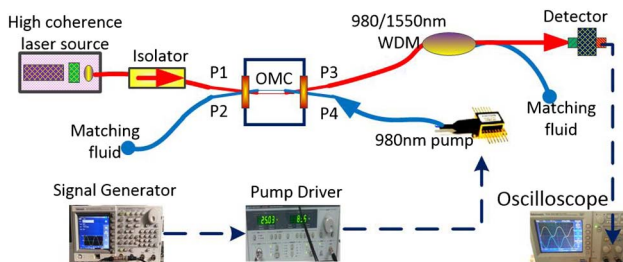
eliminating reflection at the end face. The OMC is hung inside a cube box.

Firstly, we measured the output of the 980 nm pump laser directly at the FC placed with another photodetector and an oscilloscope when a sinusoidal modulation signal with a frequency of 1 kHz and an amplitude of 160 mV was imposed on the 980 nm pump driver. We observed that the intensity of the pump light was modulated clearly, corresponding to the modulation signal. We had adjusted the modulation depth of the 980 nm pump light signal to be near 1 in the next experiments. Then, we connected the 980 nm pump laser into the system again, as shown in Fig. 4, kept the modulation signal amplitude unchanged, and measured the responses of the system at the modulation frequency range of 0.2–20 kHz. The output of the system was measured with an oscilloscope. Figure 5 shows the measured output signal under 980 nm pump laser with modulation frequencies of 1 and 20 kHz, respectively. The modulated signal is the top waveform shown in Fig. 5, and the bottom waveform in Fig. 5 is the sinusoidal modulation electrical signal. It could be seen that the modulation system can realize a synchronous stable response to a 980 nm modulated laser. In the system, we switched off the 1550 nm laser, and then the modulated signal at the output of the OMC disappeared. It proved that the 1550 nm light was modulated by the intensity-modulated 980 nm pump light. We repeated the above process by removing the 980/1550 WDM and connecting the OMC Port3 to the photodetector. The results demonstrate that by injecting 980 nm modulated pumped laser in this way the laser will not be coupled into Port3. The OMC can be integrated conveniently to the system as a modulator.

We replaced the OMC separately with a conventional 3 dB coupler and a coupler with an 8 μm tapered waist diameter, and then we could not observe the same phenomenon. The above processes have verified that the OMC could work as a modulator driven by the intensity-modulated 980 nm pump light, and it could be an all-optical modulator based on the light induced thermal effect.

To measure the responses of the OMC modulator, we sampled the output of the oscilloscope by a computer

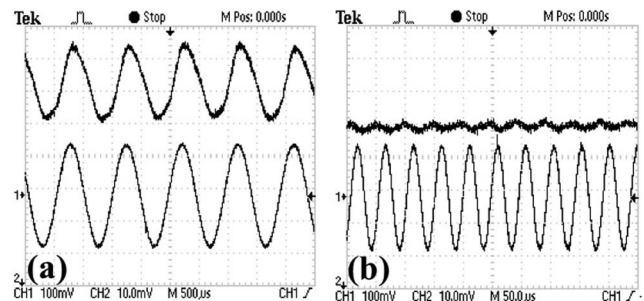Fig. 4. Schematic of the measurement system.

Fig. 5. Oscilloscope display of the output of the system (top waveform) and the modulation signal (bottom waveform): (a) 1 kHz; (b) 20 kHz.

and calculated the amplitude of modulation produced by the OMC modulator. The linear response property of the OMC modulator was measured by varying the amplitude of modulating signals imposed on the 980 nm laser driver at the frequencies of 1 and 5 kHz. The experimental results are plotted in Fig. 6, showing that the OMC modulator has good linearity with pump light power below 2.5 mW. The system modulation depth is 10.4% and 6.4% at 1 and 5 kHz, respectively, when the intensity-modulated 980 nm pump light imposed on the OMC modulator was 1 mW, and the modulation depth could reach 75% with 2.5 mW pump light, which is high enough to be used in intensity modulation applications.

The frequency responses of the OMC modulator were measured in the system. Meanwhile, the average power of the 980 nm modulated light was constant, which had been measured to be 2 mW. In order to eliminate the effects of the length, local loss of OMC, and the effects of the intensity variation of the 980 nm modulation light, we normalized the values of the measured frequency responses with the phase modulation amplitude at a frequency of 0.2 kHz. The measured data of the frequency response curves are plotted in Fig. 7. From Fig. 7, it could be seen that with the increase of modulation frequency the response decreases dramatically with a roughly inverse relation with modulation frequency. It is evident that the
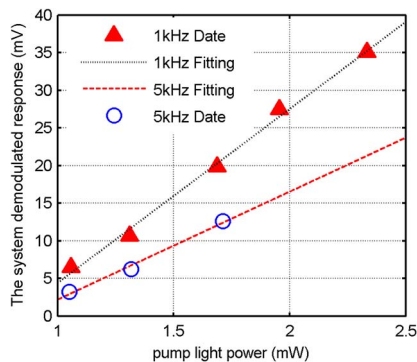

Fig. 6. Measured (dots) and fitted linear responses of the OMC modulator at 1 and 5 kHz frequencies.
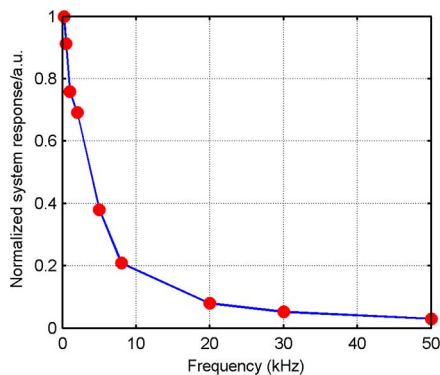

Fig. 7. Measured frequency response of the all-optical OMC modulator.
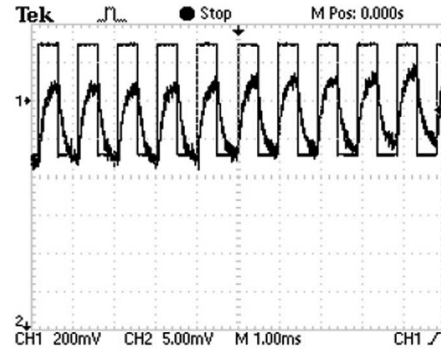

Fig. 8. Oscilloscope display of the output of the system (CH2) and the modulation signal (CH1) for square-wave modulation.

measured frequency responses are consistent with the theoretical analysis. The modulation signal has been measured up to 50 kHz.

For further understanding of the modulation response speed, the 980 nm pump laser is injected in a square-wave form. Figure 8 shows the system response result when the modulation frequency is set as 1 kHz. The result shows that the response signal has a rise time of about 500 μs. Even though the modulation speed of the demonstrated device is relatively slow, it may find applications in low frequency modulators with small power consumption.

To ensure that there is enough light extinction ratio and modulation speed, which are essential for real applications, we should optimize the structure and function design of OMCs and further increase the response speed. For example, we could add metallic or polymer coatings on a tiny waist region to enhance the nonlinear and thermal-optic effects[3–8], thus increasing the OMCs' all-optical modulation efficiency.

In conclusion, this Letter analyzes the modulation mechanisms and characteristics of thermal-optic-effect-based OMC all-optical modulators. By optimizing the design of the structure, the output intensity of 1550 nm probe light through the OMC is modulated directly by heating the coupling region with 980 nm pump light injected into the OMC. The OMC modulator shows good linear modulation responses with the intensity of the 980 nm pump light (with power below 2.5 mW), and the modulation efficiency is inversely proportional to the modulation frequency. The frequency responses of the modulator can be at 0.2–50 kHz, which may be further improved by optimizing the design of the coupler. Further works will be carried out on the modulation efficiency, the package, and the selection of the modulating light wavelength of the OMC modulator. As a passive, linear, all-optical modulator, the OMC will obtain fast development and real applications in minimized and integrated all-optical communication and sensing systems.

References

1. E. L. Wooten, K. M. Kissa, A. Yi-Yan, E. J. Murphy, D. A. Lafaw, P. F. Hallemeier, D. Maack, D. V. Attanasio, D. J. Fritz, G. J. McBrien, and D. E. Bossi, IEEE J. Sel. Top. Quantum Electron. **6**, 69 (2000).
2. M. K. Davis, M. J. F. Digonnet, and R. H. Pantell, J. Lightwave Technol. **16**, 1013 (1998).
3. A. Liu, R. Jones, L. Liao, D. Samara-Rubio, D. Rubin, O. Cohen, R. Nicolaescu, and M. Paniccia, Nature **427**, 615 (2004).
4. V. R. Almeida, C. A. Barrios, R. R. Panepucci, and M. Lipson, Nature **431**, 1081 (2004).
5. D.-J. Won, M. O. Ramirez, H. Kang, V. Gopalan, N. F. Baril, J. Calkins, J. V. Badding, and P. J. A. Sazio, Appl. Phys. Lett. **91**, 161112 (2007).
6. M. Hochberg, T. Baehr-Jones, G. Wang, M. Shearn, K. Harvard, J. Luo, B. Chen, Z. Shi, R. Lawson, P. Sullivan, A. K. Y. Jen, L. Dalton, and A. Scherer, Nat. Mater. **5**, 703 (2006).
7. D. Pacifici, H. J. Lezec, and H. A. Atwater, Nat. Photon. **1**, 402 (2007).
8. K. Nozaki, T. Tanabe, A. Shinya, S. Matsuo, T. Sato, H. Taniyama, and M. Notomi, Nat. Photon. **4**, 477 (2010).
9. L. Tong, F. Zi, X. Guo, and J. Lou, Opt. Commun. **285**, 4641 (2012).
10. M. Liu, A. Luo, W. Xu, and Z. Luo, Chin. Opt. Lett. **16**, 020008 (2018).
11. A. Sulaiman, S. W. Harun, and H. Ahmad, Chin. Opt. Lett. **12**, 021403 (2014).
12. Z. Y. Xu, Y. H. Li, and L. J. Wang, Photon. Res. **4**, 45 (2016).
13. Y. Wu, B. C. Yao, Q. Y. Feng, X. L. Cao, X. Y. Zhou, Y. J. Rao, Y. Gong, W. L. Zhang, Z. G. Wang, Y. F. Chen, and K. S. Chiang, Photon. Res. **3**, A64 (2015).
14. S. Yu, C. Meng, B. Chen, H. Wang, X. Wu, W. Liu, S. Zhang, Y. Liu, Y. Su, and L. Tong, Opt. Express **23**, 10764 (2015).
15. X. T. Gan, C. Y. Zhao, Y. D. Wang, D. Mao, L. Fang, L. Han, and J. L. Zhao, Optica **2**, 468 (2015).
16. Y. Meng, L. Deng, Z. Liu, H. Xiao, X. Guo, M. Liao, A. Guo, T. Ying, and Y. Tian, Opt. Express **25**, 18451 (2017).
17. R. Wang, D. Li, H. Wu, M. Jiang, Z. Sun, Y. Tian, J. Bai, and Z. Ren, IEEE Photon. J. **99** (2017).
18. Z. Song, Y. Yu, X. Zhang, Z. Wei, and Z. Meng, Chin. Opt. Lett. **12**, 090606 (2014).
19. Y. Jung, G. Brambilla, and D. J. Richardson, Opt Express **17**, 5273 (2009).
20. M. Ding, P. Wang, and G. Brambilla, Photon. Technol. Lett. **24**, 1209 (2012).
21. M. V. Hernández-Arriaga, M. A. Bello-Jiménez, A. Rodríguez-Cobos, R. López-Estopier, and M. V. Andrés, IEEE Sens. J. **17**, 333 (2017).
22. S. Wang, H. Yang, Y. Liao, X. Wang, and J. Wang, IEEE Photon. J. **8**, 6804209 (2016).
23. L. Sun, Y. Semenova, Q. Wu, D. Liu, J. Yuan, X. Sang, B. Yan, K. Wang, C. Yu, and G. Farrell, IEEE Photon. J. **8**, 6805407 (2016).
24. T. A. Birks and Y. W. Li, J. Lightwave Technol. **10**, 432 (1992).
25. L. Tong, Opt. Express **12**, 1025 (2004).
26. Y. Yu, X. Zhang, Z. Song, Z. Wei, and Z. Meng, Chin. Opt. Lett. **12**, 012301 (2014).
27. Y. Yu, Q. Bian, and X. Zhang, Chin. J. Lasers **45**, 0606003 (2018).